

Status of the CANGAROO-III Project

K. Nishijima^a, Y. Adachi^b, A. Asahara^c, G.V. Bicknell^d, R.W. Clay^e, Y. Doi^f,
 P.G. Edwards^g, R. Enomoto^b, S. Gunji^f, S. Hara^b, T. Hara^h, T. Hattori^a, Sei. Hayashiⁱ,
 Y. Higashi^c, R. Inoue^a, C. Itoh^j, S. Kabuki^b, F. Kajinoⁱ, H. Katagiri^c, A. Kawachi^a,
 S. Kawasaki^b, T. Kifune^k, R. Kiuchi^b, K. Konno^f, L.T. Ksenofontov^b, H. Kubo^c,
 J. Kushida^a, Y. Matsubara^l, Y. Mizumoto^m, M. Mori^b, H. Muraishiⁿ, Y. Muraki^l, T. Naito^h,
 T. Nakamori^c, D. Nishida^c, M. Ohishi^b, J.R. Patterson^e, R.J. Protheroe^e, Y. Sakamoto^o,
 M. Sato^f, S. Suzuki^p, T. Suzuki^p, D.L. Swaby^e, T. Tanimori^c, H. Tanimura^c, G.J. Thornton^e,
 K. Tsuchiya^b, S. Watanabe^c, T. Yamaokaⁱ, M. Yamazakiⁱ, S. Yanagita^p, T. Yoshida^p,
 T. Yoshikoshi^b, M. Yuasa^b, Y. Yukawa^b

(a) Department of Physics, Tokai University, Hiratsuka, Kanagawa 259-1292, Japan

(b) Institute for Cosmic Ray Research, University of Tokyo, Kashiwa, Chiba 277-8582, Japan

(c) Department of Physics, Graduate School of Science, Kyoto University, Sakyo-ku, Kyoto 606-8502, Japan

(d) Research School of Astronomy and Astrophysics, Australian National University, ACT 2611, Australia

(e) Department of Physics and Mathematical Physics, University of Adelaide, SA 5005, Australia

(f) Department of Physics, Yamagata University, Yamagata, Yamagata 990-8560, Japan

(g) Institute of Space and Astronautical Science, Sagamihara, Kanagawa 229-8510, Japan

(h) Faculty of Management Information, Yamanashi Gakuin University, Kofu, Yamanashi 400-8575, Japan

(i) Department of Physics, Konan University, Kobe, Hyogo 658-8501, Japan

(j) Ibaraki Prefectural University of Health Sciences, Ami, Ibaraki 300-0394, Japan

(k) Faculty of Engineering, Shinshu University, Nagano, Nagano 480-8553, Japan

(l) Solar-Terrestrial Environment Laboratory, Nagoya University, Nagoya, Aichi 464-8602, Japan

(m) National Astronomical Observatory of Japan, Mitaka, Tokyo 181-8588, Japan

(n) School of Allied Health Sciences, Kitasato University, Sagamihara, Kanagawa 228-8555, Japan

(o) Course in Physical and Mathematical Science, Graduate School of Science and Technology, Tokai University Hiratsuka, Kanagawa 259-1292, Japan

(p) Faculty of Science, Ibaraki University, Mito, Ibaraki 310-8512, Japan

Presenter: K. Nishijima (kyoshi@tkikam.sp.u-toaki.ac.jp), jap-nishijima-K-abs1-og27-oral

The CANGAROO-III telescope array for sub-TeV gamma-ray astronomy consists of four 10 m atmospheric Cherenkov telescopes. The construction of the fourth telescope was completed in summer, 2003 and a stereoscopic observation with a local trigger system was started in March 2004. In December 2004, a global stereo trigger system was installed and real-time stereoscopic operation was started. The telescope performance is checked using star images taken by a CCD camera, and analyses of stereo data and tuning of Monte Carlo simulations has been carried by use of local muons and observations data of the Crab Nebula.

1. Introduction

Fig. 1 shows the CANGAROO-III telescope array, which is located near Woomera, South Australia (136°47' E, 31°06' S, 160m altitude). These telescopes are placed at the corners of a diamond as shown at the right-hand side of Fig. 1. Stereo observations with the first (T1) and the second (T2) telescopes started in December, 2002. The third (T3) and fourth (T4) telescopes were added in July 2003 and March 2004, respectively. Until November 2004, data acquisition was triggered locally and events were recorded separately for each telescope. Stereo events were extracted during off-line analysis. In December 2004, we upgraded the trigger system to a global one and started DAQ with a stereoscopic trigger.

Unfortunately, the oldest telescope, T1, has a higher energy threshold and poorer efficiency for stereo

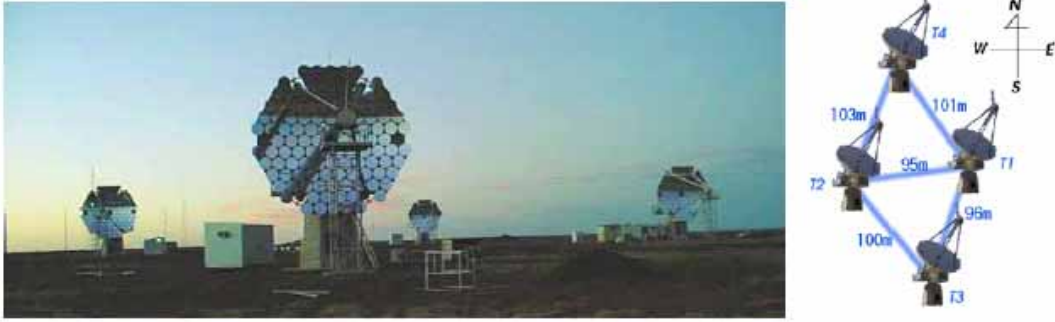


Figure 1. The CANGAROO-III telescope system near Woomera, South Australia viewed from the south. The drawing on the right shows the arrangement of the four telescopes.

observations, so the operation of T1 has been stopped.

Here we describe briefly the current status of the CANGAROO-III project including checks of telescope performance using muon events and the global trigger system mentioned above. Results of the observations of some individual targets are reported elsewhere in this conference, which are summarized in Table 1.

Table 1. Observed targets, results of which will be reported in this conference

Target	Obs. Time (hrs)	Ref.	Target	Obs. Time (hrs)	Ref.
Crab	53.9	[1]	Galactic disc	9.3	[3]
RXJ 0852.0-4622	46.1	[2]	Mrk 421	11.3	[4]
SN1006	40.7		PKS 2155-304	41.0	
PSR 1706-44	36.9		Cen A	21.7	[5]

2. The CANGAROO-III Telescopes

The CANGAROO-III telescopes have parabolic reflectors of 10 m diameter with an 8 m focal length. Each consists of 114 small spherical mirrors of 80 cm diameter, which are made of CFRP (T1) [6] and GFRP (T2, T3 and T4). The imaging cameras of T2, T3 and T4 have 427 pixels of 0.17° size and a field of view of 4° [7], whereas T1's has 552 pixels with a field of view of 2.7° . These telescopes use alt-azimuth mounts and the tracking accuracy has been measured by observing star positions using a CCD camera. The RMS deviation from the star position is about 0.013° which is sufficiently small compared to the pixel size. Also, spot sizes have been measured by observing star images on the camera using a CCD camera. The FWHM point spread functions of T1, T2, T3, and T4 are 0.20° , 0.21° , 0.14° , and 0.16° , respectively.

Transparency of the atmosphere at the telescope site was evaluated by observing the extinction of star light, and the night sky background was measured using both the CCD camera and the observed data. These results are shown elsewhere in this conference [8].

3. Muon Events

In order to understand the performance of the telescopes and tune the Monte Carlo simulations, muon events are used. We select images as clear muon events by requiring that each image forms a good ring shape with one or more clusters and has an *Arclength* longer than 2° . Fig. 2 shows χ^2 distributions for ring fitting (left

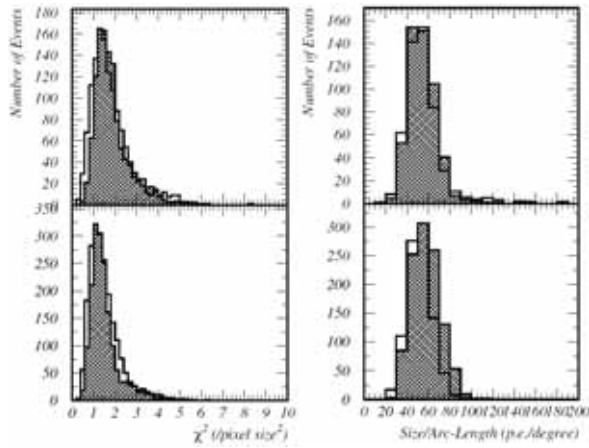


Figure 2. Observed muon parameters (histogram) compared with Monte Carlo simulations (hatched). Left and right panels show χ^2 distributions for ring fitting and distributions of *Size/Arclength*, respectively. Upper and bottom panels are shown for T2 and T3, respectively.

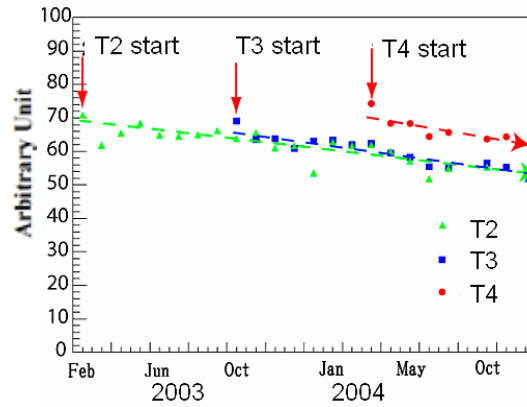


Figure 3. Time variation of the relative light collection efficiency for each telescope, which is proportional to *Size/Arclength*

panels) and distributions of the ratio of *Size/Arclength* (right), for T2 (upper) and T3 (bottom), respectively, compared with the Monte Carlo simulation data. The χ^2 for ring fitting is sensitive to the spot size, while the *Size/Arclength* is roughly proportional to the total light collection efficiency. All panels in Fig. 2 show good consistency between the observed data and the Monte Carlo simulations. The *Size/Arclength* can be used to monitor the total light conversion efficiency over long periods. Fig. 3 shows the time variation of the relative light collection efficiency for T2 (closed triangles), T3 (closed squares), and T4 (closed circles), respectively. They are gradually decreasing with a rate of about 5 %/year, which is mainly caused by the degradation of the mirrors due to the environment. The results of a study of the reflectivity of mirrors [8] and more details of a study of muon events [9] are reported elsewhere in this conference.

4. Global Trigger

As mentioned above, only T2, T3 and T4 are used for the stereo trigger. For each telescope, when the number of hit pixels (*nhit*), each of which received photoelectrons (*lsum*) over a certain threshold, exceeds a set value, data from the ADC, TDC and GPS are kept for 5 μ sec and at the same time a local trigger is sent to the stereo trigger system through an optical link. In the stereo trigger system, determination of stereo events is done by requiring any two or three local trigger signals coinciding with each other for at least 10 nsec within a 650 nsec time window considering the geometrical time delay which depends on the arrival direction of Cherenkov light. When a stereo event is detected, a global trigger signal is generated and the event number and timing information are recorded. Then, the generated global trigger signal and event number are sent to each telescope. At each telescope, when the global trigger signal from stereo trigger system is received within 5 μ sec, ADC and TDC data are read out and recorded. If not, the data for that event are cleared, and the DAQ and local trigger system are reset for the next event.

We investigate the *lsum* threshold dependence of the trigger rate for fixed *nhit* threshold. For example, for relatively dark sky near the zenith, the recorded rate at T4 in the case of a fixed *nhit* threshold of 3 is reduced by a factor 30 for the *lsum* threshold of 6 p.e. which corresponds to the case of the previous local trigger condition, and is two orders of magnitude less for 4.7 p.e. compared with a local trigger rate. Endurance tests of the DAQ for high trigger rates have been performed. Fig. 4 shows the live time against the local trigger

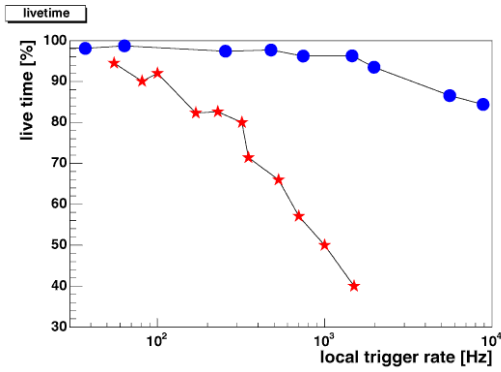


Figure 4. The fraction of live time against the local trigger rate. Closed circles indicate for local trigger with global trigger and stars indicate for previous local trigger.

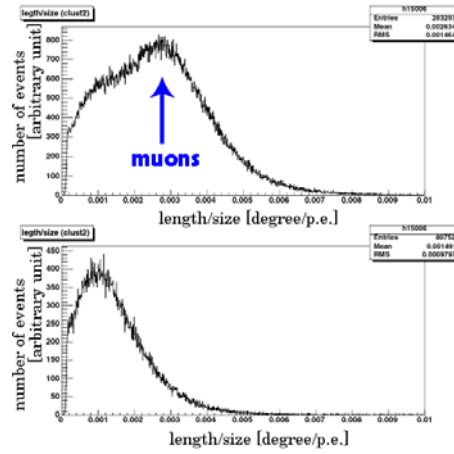


Figure 5. *length/size* distributions without (upper) and with (bottom) the global trigger.

rate. From this figure, a fraction of live time of higher than 90% is kept for less than about 5 kHz, which corresponds to about 50 times higher rate than the previous local trigger rate. This is because the global trigger system abandons most of the local triggered events due to the night sky background or muons, and the resultant dead time is reduced by a factor of 100. Fig. 5 shows a comparison of the *length/size* distributions before and after the introduction of the global trigger system. We can see the peak caused by muons is almost completely removed by the global trigger. So, by introducing the global trigger system, muon events are clearly removed and the hardware threshold of DAQ can be lowered, and thus the energy threshold of detectable gamma-rays becomes 20 – 30 % lower than before. Current analysis threshold energy is around 600 GeV.

5. Summary

We have been carrying out stereo observations of sub-TeV gamma-rays with four telescopes since March 2004. The global stereo trigger system was installed in December 2004, and is working successfully to reduce local muon events. The performance of telescopes is being checked by observing star images using a CCD camera, and stereo analyses including tuning of the Monte Carlo simulations are being calibrated using muon events.

References

- [1] T. Nakamori et al., 29th ICRC, Pune (2005).
- [2] T. Tanimori et al., 29th ICRC, Pune (2005).
- [3] M. Ohishi et al., 29th ICRC, Pune (2005).
- [4] Y. Sakamoto et al., 29th ICRC, Pune (2005).
- [5] S. Kabuki et al., 29th ICRC, Pune (2005).
- [6] A. Kawachi et al., *Astropart. Phys.* 14, 261 (2001).
- [7] S. Kabuki et al., *Nucl. Instr. & Meth. A* 500, 318 (2003).
- [8] R. Kiuchi et al., 29th ICRC, Pune (2005).
- [9] T. Yoshikoshi et al., 29th ICRC, Pune (2005).